

Thermal Properties, Thermal Shock, and Thermal Cycling Behavior of Lanthanum Zirconate-Based Thermal Barrier Coatings



XINGYE GUO, ZHE LU, YEON-GIL JUNG, LI LI, JAMES KNAPP, and JING ZHANG

Lanthanum zirconate ($\text{La}_2\text{Zr}_2\text{O}_7$) coatings are newly proposed thermal barrier coating (TBC) systems which exhibit lower thermal conductivity and potentially higher thermal stability compared to other traditional thermal barrier systems. In this work, $\text{La}_2\text{Zr}_2\text{O}_7$ and 8 wt pct yttria stabilized zirconia (8YSZ) single-layer and double-layer TBC systems were deposited using the air plasma spray technique. Thermal properties of the coatings were measured. Furnace heat treatment and jet engine thermal shock tests were implemented to evaluate coating performance during thermal cycling. The measured average thermal conductivity of porous $\text{La}_2\text{Zr}_2\text{O}_7$ coating ranged from 0.59 to 0.68 W/m/K in the temperature range of 297 K to 1172 K (24 °C to 899 °C), which was approximately 25 pct lower than that of porous 8YSZ (0.84 to 0.87 W/m/K) in the same temperature range. The coefficients of thermal expansion values of $\text{La}_2\text{Zr}_2\text{O}_7$ were approximately 9 to $10 \times 10^{-6}/\text{K}$ from 400 K to 1600 K (127 °C to 1327 °C), which were about 10 pct lower than those of porous 8YSZ. The double-layer coating system consisting of the porous 8YSZ and $\text{La}_2\text{Zr}_2\text{O}_7$ layers had better thermal shock resistance and thermal cycling performance than those of single-layer $\text{La}_2\text{Zr}_2\text{O}_7$ coating and double-layer coating with dense 8YSZ and $\text{La}_2\text{Zr}_2\text{O}_7$ coatings. This study suggests that porous 8YSZ coating can be employed as a buffer layer in $\text{La}_2\text{Zr}_2\text{O}_7$ -based TBC systems to improve the overall coating durability during service.

DOI: 10.1007/s40553-016-0070-4

© ASM International (ASM) and The Minerals, Metals & Materials Society (TMS) 2016

I. INTRODUCTION

REFRACTORY oxide ceramic materials have been deposited on top of bond-coated metallic components as thermal barrier coatings (TBCs) in gas turbine engines, *e.g.*, combustors, rotating blades, stationary guide vanes, blade outer air seals, and afterburners in the tail section of jet engines, *etc.* TBCs are critical to the performance of gas turbine engines in terms of enabling engines to operate at temperatures above the melting points of metallic components.^[1–5] With the benefit of high operation temperatures, the energy efficiency of the gas turbine can be greatly increased. Conventional TBCs are 7 to 8 wt pct yttria stabilized zirconia (8YSZ) coatings deposited by air plasma spraying (APS) or electron beam physical vapor deposition (EB-PVD). As the coating is deposited, the non-transformable tetragonal (T') forms upon rapidly quenching. At elevated temperatures above 1473 K (1200 °C) for a

sufficient amount of time, transformable tetragonal (T) and cubic (F) phases form. The transformable tetragonal (T) is capable of forming the monoclinic (M) phase upon cooling due to the partitioning of yttria at high temperatures, which causes a 3 to 5 pct volume change that is detrimental to coating life.^[6]

Modern gas turbine engines demand advanced TBCs that can be employed at high operating temperatures above 1473 K (1200 °C). Lanthanum zirconate ($\text{La}_2\text{Zr}_2\text{O}_7$, LZ) has been proposed as a promising advanced TBC material to substitute for 8YSZ.^[7] LZ has no phase change from room temperature to its melting point, which is 2573 K (2300 °C). Compared with YSZ, it has a lower thermal conductivity (1.5 W/m/K for bulk LZ and 2.1 to 2.2 W/m/K for bulk YSZ), lower sintering ability, and lower coefficient of thermal expansions (CTEs, 9.1 to $9.7 \times 10^{-6} \text{ K}^{-1}$ for LZ and 10.5 to $11.5 \times 10^{-6} \text{ K}^{-1}$ for YSZ).^[7] The high-temperature phase stability of LZ has been studied using synchrotron X-ray diffraction (XRD) at Argonne National Laboratory.^[8–10] The results showed no phase transformation in the temperature range of 303 K to 1673 K (30 °C to 1400 °C).^[8] Vassen *et al.* studied the thermal cycling behavior of TBCs with single-layer and double-layer coatings (8YSZ sublayer and LZ top layer) in the temperature range between 1473 K and 1723 K (1200 °C and 1450 °C). The results showed that the single-layer LZ coatings had a rather poor thermal cycling performance at temperatures above 1573 K (1300 °C), and the double-layer systems showed similar

XINGYE GUO, Ph.D. Candidate, and JING ZHANG, Associate Professor, are with the Department of Mechanical Engineering, Indiana University–Purdue University Indianapolis, Indianapolis, IN 46202. Contact e-mail: jz29@iupui.edu ZHE LU, Postdoctoral Researcher, and YEON-GIL JUNG, Professor, are with the School of Materials Science and Engineering, Changwon National University, Changwon, Gyeongnam 641-773, Republic of Korea. LI LI, Project Manager, and JAMES KNAPP, Director, are with Praxair Surface Technologies Inc., Indianapolis, IN 46222.

Manuscript submitted June 4, 2015.

Article published online March 29, 2016

results to 8YSZ coatings at temperatures below 1573 K (1300 °C).^[11] Jung *et al.* investigated the thermal cycling behavior of 8YSZ TBC systems, indicating that the microstructural features were an important factor, and it was necessary to optimize the porosity in thick coatings.^[12]

The present study focuses on the thermal performance of LZ-based TBCs, where data are still scarce. In this investigation, the thermal conductivity and CTEs of LZ coating were measured. The thermal shock and thermal cycling behavior of the single- and double-layered LZ-based TBCs were investigated using both furnace heat treatment and jet engine thermal shock (JETS) tests. The results are compared with conventional 8YSZ coatings.

II. EXPERIMENTAL METHOD

A. Sample Preparation

The TBC systems in this work included a metallic substrate, a metallic bond coat layer, and one or two ceramic top coat layers. Haynes 188 superalloy (Haynes International, Kokomo, IN) buttons with a diameter of 25.4 mm (1 in.) and a thickness of 3.175 mm (1/8 in.) were used as the substrates in this study. NiCrAlY powder, Ni-211 (Praxair Surface Technologies, Indianapolis, IN, with a chemistry 61.5 wt pct, Cr 21.12 wt pct, Al 9.94 wt pct, Y 1.02 wt pct^[13]), was selected as a bond coat feedstock. The bond coat thickness was 180 to 200 μm . AMPERIT 825.001 and AMPERIT 827.006 (HC Starck, Munich, Germany) were selected powders to produce the dense and porous 8YSZ. LAO-109-1 (Praxair Surface Technologies, Indianapolis, IN) was the powder used to produce the LZ coatings. All coating spraying was conducted at Praxair Surface Technologies, Inc. using a proprietary shrouded plasma technique.

Two different types of double-layer TBC samples were deposited: LZ coating on a porous 8YSZ layer and LZ coating on a dense 8YSZ layer. Additionally, two types of single-layer TBC samples, single-layer LZ and single-layer porous 8YSZ, were produced for comparison purposes. All prepared TBC samples are listed in Table I.

B. Testing Methods

The density measurement for LZ top coat was conducted using 432 μm thick free standing coatings produced by depositing the LZ top coat onto aluminum substrates, which were then leached away using diluted

NaOH solution. The density was measured following the ASTM standard B328-94, which is based on the Archimedes' principle. The measurement apparatus includes an analytical balance (Mettler AE240, Switzerland) and a density determination kit (Denver Instrument, density kit, Arvada, CO).

Thermal diffusivity was measured by using a laser flash diffusivity system DLF 1200 (TA Instrument, Delaware). Thermal conductivity, k , was then calculated from thermal diffusivity D_{th} (measured), specific heat capacity C_p (from literature^[6]), and density ρ (measured):

$$k = D_{\text{th}} \cdot C_p \cdot \rho. \quad [1]$$

The CTEs (sample size 5 mm in width, 25 mm in length and 0.43 mm in thickness) were measured by using a BAEHR dilatometer DIL 802 (now belonging to TA instrument, Delaware) at temperatures ranging from room temperature to 1673 K (1400 °C).

Furnace heat treatment tests were conducted at 1353 K (1080 °C) for 4 hours in an argon atmosphere using round button samples with a diameter of 25.4 mm (1 in.). Additionally, JETS tests were conducted to investigate the thermal shock and thermal cycling performance. During JETS tests, the TBC samples were heated to 1505 K (1232 °C) at the center for 20 seconds and then were cooled by compressed N_2 for 20 seconds, followed by ambient cooling for 40 seconds. The heating and cooling cycle was repeated until the TBC samples failed. The failure criterion in the JETS tests was more than 20 pct spallation of the TBC surface.^[14] Both the front and back side temperatures were measured during the test through two-color pyrometers to investigate the temperature gradient across sample thickness. The TBC samples were sectioned and polished according to the ASTM standard E1920-30 to examine their microstructures using a scanning electron microscope (SEM, JEOL Model JSM-5610, Japan).

III. RESULTS AND DISCUSSION

A. Porosity, Thermal Conductivity, and Coefficient of Thermal Expansion

The measured average density and porosity for the LZ layer were 5.31 g/cm^3 and 11.54 pct, respectively. Porosities in the dense 8YSZ and porous 8YSZ layers were 7.24 and 15.95 pct, respectively. In order to study the thermal shock and thermal cycling behaviors of the LZ coating, thermal properties, such as thermal conductivity and CTE, were compared in the 8YSZ and LZ

Table I. List of TBC Samples

Type of TBC	Substrate	Bond Coat	Top Coats	Thickness
1	Haynes 188	NiCrAlY	single-layer $\text{La}_2\text{Zr}_2\text{O}_7$	424 μm
2	Haynes 188	NiCrAlY	porous 8YSZ + $\text{La}_2\text{Zr}_2\text{O}_7$	138 + 305 μm
3	Haynes 188	NiCrAlY	dense 8YSZ + $\text{La}_2\text{Zr}_2\text{O}_7$	140 + 292 μm
4	Haynes 188	NiCrAlY	single-layer porous 8YSZ	452 μm

coating samples. The thermal conductivities of the as-sprayed single-layer porous LZ and porous 8YSZ coatings are plotted in Figure 1. Three thermal conductivity measurements were conducted for the LZ coatings at each temperature setting [297 K, 377 K, 477 K, 579 K, 676 K, 776 K, 874 K, 974 K, 1072 K, and 1172 K (24 °C, 104 °C, 204 °C, 306 °C, 403 °C, 503 °C, 601 °C, 701 °C, 799 °C, and 899 °C)]. The measured average thermal conductivity of the LZ was about 0.59 to 0.68 W/m/K in the temperature range of 297 K to 1172 K (24 °C to 899 °C), which was about 25 pct lower than that of the porous 8YSZ (0.84 to 0.87 W/m/K) in the same temperature range.

The CTE values measured for the LZ coating employed in this study are shown in Figure 2. The CTE values of the LZ were about 9 to $10 \times 10^{-6} \text{ K}^{-1}$ from 400 K to 1600 K (127 °C to 1327 °C), which were very close to the reported literature data.^[15–17] The CTE values of the LZ were about 10 pct lower than those of the 8YSZ, which were 10 to $11 \times 10^{-6} \text{ K}^{-1}$ in the same temperature range.^[7,18] Due to the difference of CTE between the 8YSZ and the LZ, a thermal mismatch could be generated at the interface between the 8YSZ sublayer and the LZ top layer during the thermal shock and thermal cycling tests. As the NiCrAlY bond coat has much higher CTEs (about $15 \times 10^{-6} \text{ K}^{-1}$ at 1273 K) than the 8YSZ,^[13] a larger thermal mismatch between the 8YSZ sublayer and the LZ top layer can be generated during thermal shock and thermal cycling tests.

Thermal residual stresses were generated in each TBC layer due to different CTEs among the bond coat, the 8YSZ, and the LZ during heating and cooling processes. When the coatings were cooled from high temperatures, the volume shrinkages of the substrate and the bond coat were larger than that of the top coats, due to the higher CTEs. Considering displacement compatibility, compressive stress was created in the ceramic top coat and tensile stress in the bond coat and the substrate. However, when the coating sample was heated, tensile

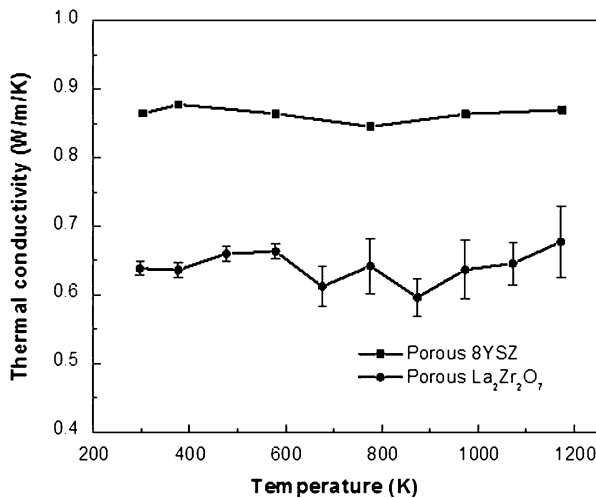


Fig. 1—Thermal conductivities of LZ and 8YSZ as a function of temperature. The lines serve as a guide for the eye.

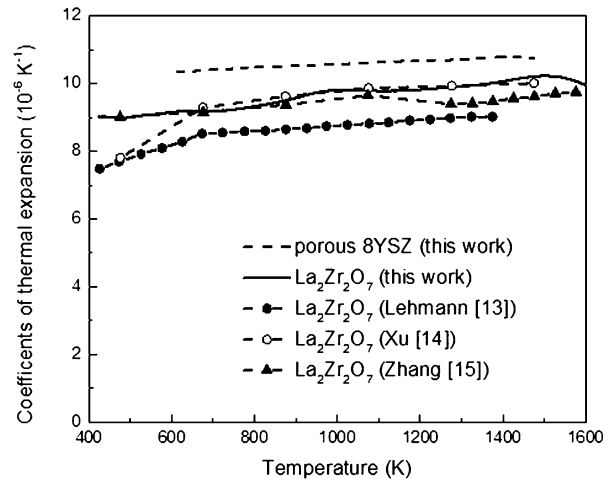


Fig. 2—Coefficient of thermal expansion values of LZ and 8YSZ as a function of temperature.

stress was generated in the ceramic top coat and compressive stress in the bond coat and the substrate.

The stress differences of the single- and double-layer TBCs can be estimated using an elastic analytical model.^[19–21] The calculated stress distributions across the coating thickness of the four TBC samples are shown in Figure 3. The results indicate that the stress difference between the top and bond coats in the single-layer LZ sample was larger than that of the single-layer porous 8YSZ sample. However, although the stress differences between the two double-layer coatings were similar, they were much smaller than those between the single-layer LZ coatings.

B. Furnace Heat Treatment

The optical images of the TBC samples before and after the furnace heat treatment are summarized in Figure 4. After furnace heat treatment for 4 hours, the single-layer LZ coating (Figure 4(a)) and the double-layer coating with the dense 8YSZ and LZ layers

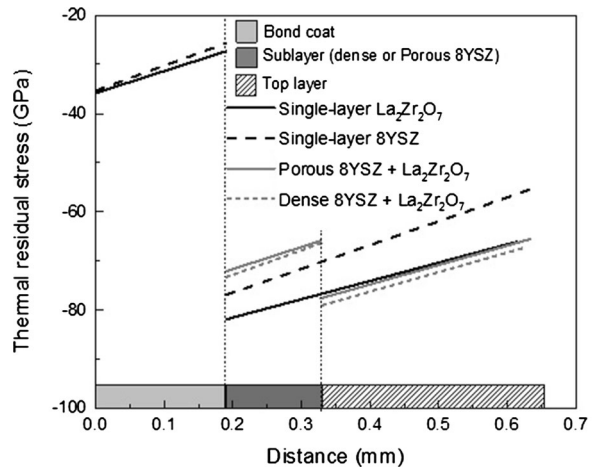


Fig. 3—Calculated residual stress distributions as a function of thickness in four TBC samples.

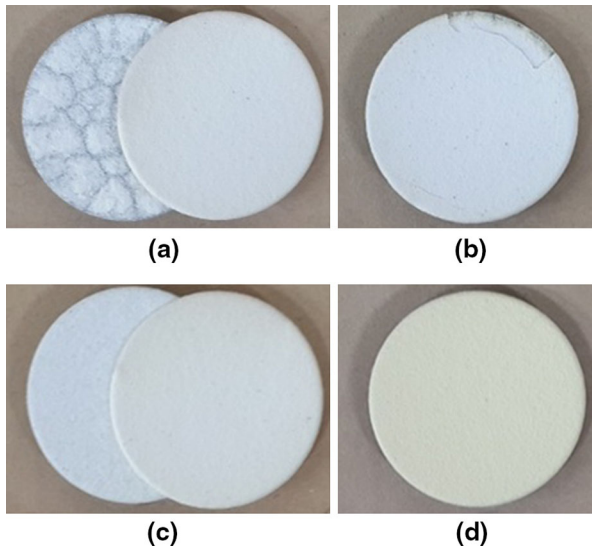


Fig. 4—Optical images of the TBC samples after furnace heat treatment: (a) single-layer LZ coating, (b) double-layer coating with porous 8YSZ and LZ, (c) double-layer coating with dense 8YSZ and LZ, and (d) single-layer porous 8YSZ coating.

(Figure 4(c)) were completely delaminated. One of the main reasons for the failure was the CTE differences among the bond coat, the 8YSZ layer, and the LZ layer. In the isothermal heating process, volume change due to the thermal expansion mismatch between the bond coat and the LZ layer led to high thermal residual stresses, which initiated cracks in ceramic top coats, as indicated in the calculated stress distribution in Figure 3. Additionally, the fracture toughness of LZ is $\sim 1.1 \text{ MPa m}^{1/2}$, which is much lower than that of 8YSZ ($2.0 \text{ MPa m}^{1/2}$).^[6,22] As a result, cracks tended to be extended inside the LZ coating layer in the early stage of heat treatment. The failure ultimately occurred in the LZ coating layer due to its low fracture toughness and the CTE mismatch between the bond coat and the LZ layer or between the LZ and the 8YSZ layers. In contrast with the finding for the dense 8YSZ and LZ coating (Figure 4(c)), the double-layer coating with the porous 8YSZ and LZ layers was partially cracked on the edge, which only took up about 10 pct of the coated area, as shown in Figure 4(b). As the porosity of the porous 8YSZ coating was more than two times higher than that of the dense 8YSZ coating, the porous 8YSZ coating had greater compliance to accommodate the

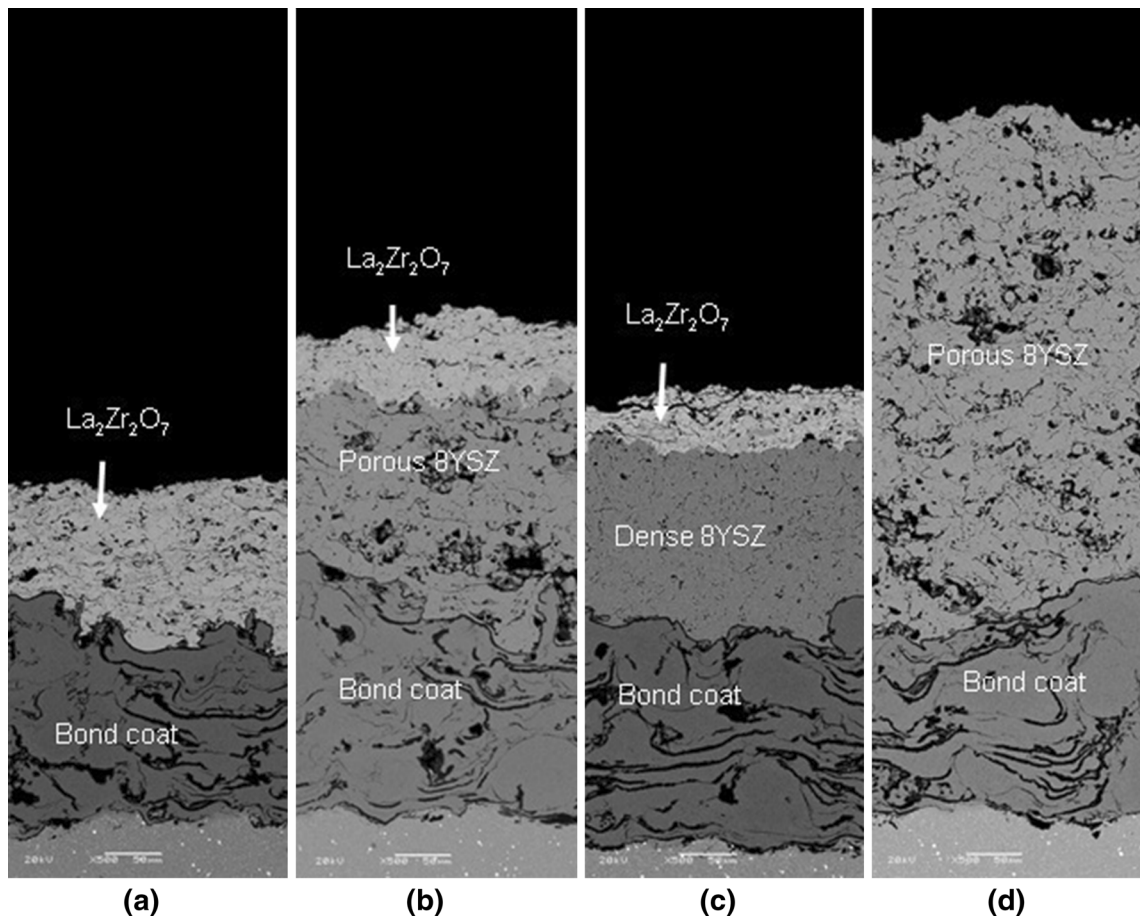


Fig. 5—SEM images of the cross-sectional view of the TBC samples after furnace heat treatment: (a) fully delaminated single-layer LZ coating, (b) edge delaminated double-layer coating with porous 8YSZ and LZ, (c) fully delaminated double-layer coating with dense 8YSZ and LZ, and (d) single-layer porous 8YSZ coating.

Table II. Summary of the Number of Cycles and Final Status in JETS Tests

	Single-Layer $\text{La}_2\text{Zr}_2\text{O}_7$	Porous $8\text{YSZ} + \text{La}_2\text{Zr}_2\text{O}_7$	Dense $8\text{YSZ} + \text{La}_2\text{Zr}_2\text{O}_7$	Single-Layer Porous 8YSZ
Number of cycles before complete delamination	25	>2000	885	>2000
Failure status	complete delaminated	edge delaminated	complete delaminated	intact

volume mismatch caused by the CTE differences, so the top coat with the porous 8YSZ and LZ coatings could survive in the heat treatment. However, the low compatibility of the dense 8YSZ coating led to its complete failure in the heat treatment. As shown in Figure 4(d), the single-layer porous 8YSZ coating was in good condition after heat treatment for 4 hours, suggesting the porous 8YSZ layer has good adhesion in TBC systems.

Figure 5 shows the SEM images of the cross-sectional view of TBC microstructures after heat treatment for 4 hours. Except for the single-layer porous 8YSZ coating (Figure 5(d)), delamination in all of the samples occurred within the LZ layer. Therefore, CTE difference should not be the only reason for delamination of the single-layer LZ coating. The occurrence of cracks is likely related to fracture toughness.^[23] Delamination can more easily occur in the single-layer LZ coating due to the low fracture toughness of LZ. Failure in the LZ coating is likely caused by a combination of its low fracture toughness and high stresses created by CTE mismatch. Levi *et al.* proposed that elastic energy played a critical role in TBC systems to determine the lifetime of coating.^[24] When the elastic energy reaches the critical energy value, delamination occurs. This elastic energy can be estimated using coating thickness, Young's modulus, and CTE.^[24] The cause of delamination in the double-layer coating with the dense 8YSZ and LZ is likely similar to the single-layer LZ coating, namely a combined effect of both CTE difference and low fracture toughness of LZ.

C. Jet Engine Thermal Shock Test

The number of cycles to failure and final top coat status after the JETS tests are summarized in Table II. During the JETS tests, the single-layer LZ coating was completely delaminated within 25 cycles, and the double-layer coating with the dense 8YSZ and the LZ was completely delaminated in about 885 cycles. Delamination happened near the interface between the dense 8YSZ layer and the LZ layer in the double-layer coating. However, the double-layer coating with the porous 8YSZ and LZ was only partially delaminated at edges after 2000 cycles, and the cracked edge area took up about 20 pct of the total area of the top coat. In the remaining area, the top coat of LZ was still bonded with the porous 8YSZ layer. The double-layer coating with the porous 8YSZ and LZ had a better performance than other LZ-based coatings. The single-layer porous 8YSZ coating was intact after 2000 cycles.

The optical images of the TBC samples after the JETS tests are shown in Figure 6. The single-layer LZ coating sample is shown in Figure 6(a) in which the LZ top coat

was completely delaminated from the bond coat. Only the bond coat remained. The double-layer coating with the dense 8YSZ and LZ is shown in Figure 6(c). In this figure, the delaminated LZ coating fragments were laid on the top surface, although it already detached from the dense 8YSZ layer. The bright area is the dense 8YSZ layer, and the dark gray region is the LZ layer. After the JETS tests, only the dense 8YSZ layer was left on the substrate. The LZ top coat was totally lost during the JETS tests. Delamination occurred between the 8YSZ and LZ layers. The single-layer porous 8YSZ coating is shown in Figure 6(d). The 8YSZ top coat was almost intact after 2000 cycles, suggesting good thermal shock resistance. The three black marks on the edge of the samples in Figures 6(a) and (d) were caused by sample holding clips. The double-layer coating with the porous 8YSZ and LZ is shown in Figure 6(b). The coating survived after the JETS tests with cracks on the edge of LZ top coat. The double-layer coating with the porous 8YSZ and LZ showed a considerably better performance than the single-layer LZ coating and the double-layer coating with the dense 8YSZ and LZ. Heating and cooling cycles led to the thermal residual stresses in

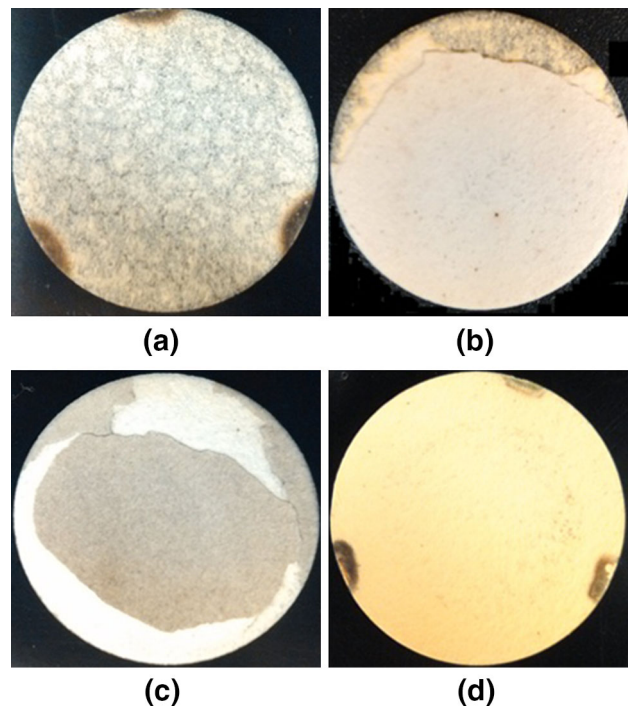


Fig. 6—Optical images of the TBC samples after JETS tests: (a) single-layer coating with LZ, (b) double-layer coating with porous 8YSZ and LZ, (c) double-layer coating with dense 8YSZ and LZ, and (d) single-layer porous 8YSZ coating.

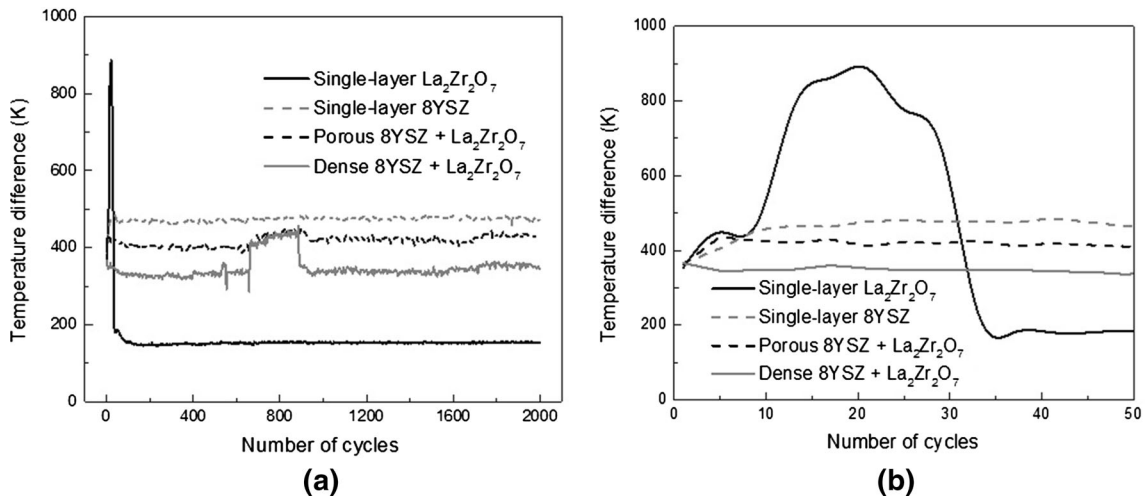


Fig. 7—Average temperature differences between the front and back sides of TBC samples during JETS tests: (a) number of cycles from 0 to 2000 and (b) number of cycles from 0 to 50.

TBC systems. The stress levels are proportional to the distance from the interface, as shown in Figure 3.^[6] For the double-layer coating with the porous 8YSZ and the LZ, the stress level at the interface between the 8YSZ and LZ layers was less than that at the interface between the 8YSZ and the bond coat.

The temperature differences between the front and back surfaces of the samples during the JETS tests are shown in Figure 7. Figure 7(a) shows the temperature difference in the cycle range from 0 to 2000, and Figure 7(b) shows the temperature difference in the cycle range from 0 to 50. As shown in Figure 7(a), the curve of double-layer coating with the dense 8YSZ and LZ showed a sudden temperature change between 660 and 885 cycles, which is an evidence of delamination. However, the double-layer coating with the porous 8YSZ and LZ, including the single-layer porous 8YSZ coating, did not show a large temperature change, suggesting that the double-layer coating with the porous 8YSZ and LZ had a similar performance in the JETS tests as that of 8YSZ. However, the double-layer coating with the porous 8YSZ and LZ showed a smaller temperature drop (~56 K on average) than the single-layer 8YSZ coating, although thermal conductivity of the as-sprayed single-layer 8YSZ coating is higher than that of the single layer LZ coating. In the JETS tests, the temperature drops of the single-layer and double-layer coatings are not simply related to the thermal conductivities of as-sprayed coatings. The temperature drops of the single layer porous 8YSZ coating can be higher than those of the double-layer coatings with 8YSZ and LZ, due to the porosity difference, the interface roughness, sintering, and thermal conductivity change in the JETS tests. In addition, the 8YSZ single-layer coating was thicker than the double-layer coatings, so the temperature drops in the single-layer 8YSZ coating can be larger than those of double-layer coatings.

As shown in Figure 7(b), the temperature differences of the single-layer LZ coating bumped up after 10 cycles

and then dropped after 25 cycles. The gaps between the top and bond coats caused the increase of front-back surface temperature differences, indicating that the LZ top coat partially delaminated from the bond coat after 10 cycles. The top surface temperature of single-layer LZ coating reached to 2032 K (1759 °C) after 13 cycles due to accumulation of heat. As the top coat delaminated after 25 cycles, the bond coat and substrate were exposed to the JETS flame directly, causing a reduced temperature difference, as shown in Figure 7(b).

With the current coating architectures, it seems that LZ-based coatings do not have the same performance as the single-layer porous 8YSZ coating in the JETS and the furnace heat treatment tests. However, as suggested in this work, the thermal cycle and thermal shock performance of the LZ-based coatings can be improved by properly designed coating architectures, for example, the double-layer coating with porous 8YSZ buffer layer and LZ top layer. For the LZ-based TBCs, there are two ways to make further improvement: (1) make the LZ layer more porous to further reduce the thermal conductivity and (2) redesign the architecture with functionally graded structure. We have on-going effort of design and fabrication of LZ-8YSZ composite coatings. It is expected that the porous 8YSZ and LZ multilayer coating with properly tuned porosity and thickness can be a good choice for future TBC systems.

IV. CONCLUSIONS

In this work, the selected TBC systems with LZ coatings, both single-layer and double-layer coatings, were fabricated, and their basic thermal properties, thermal shock, and thermal cycling behavior were characterized. The conclusions are summarized as follows:

1. The measured average thermal conductivity of single-layer LZ coating is 0.59 to 0.68 W/m/K in the temperature range of 297 K to 1172 K (24 °C to

899 °C), which is ~25 pct lower than that of single-layer porous 8YSZ coating in the same temperature range.

2. The CTE values of LZ coating are approximately 9 to $10 \times 10^{-6} \text{ K}^{-1}$ in the temperature range of 400 K to 1600 K (127 °C to 1327 °C). However, the CTE values of LZ are about 10 pct lower than those of 8YSZ in the same temperature range. The large CTE difference between the bond coat and the LZ leads to large thermal and residual stresses, which is one of the main reasons for the failure of the single-layer LZ coating.
3. Both furnace heat treatment and JETS tests show that the double-layer coating with porous 8YSZ and LZ layers has better thermal shock and thermal cycling performances than the single-layer LZ coating and the double-layer coating with the dense 8YSZ and the LZ layers. The results suggest that the porous 8YSZ can be used as a buffer layer for LZ-based TBC systems to improve the durability during service.

ACKNOWLEDGMENTS

This work was supported by the National Research Foundation of Korea (NRF) Grant funded by the Korean Government (MEST) (2011-0030058), by the Power Generation & Electricity Delivery of the Korea Institute of Energy Technology Evaluation and Planning (KETEP) Grants funded by the Korea Ministry of Knowledge Economy (2013-101010-170C), by Changwon National University in 2015 ~ 2016, and by the financial support provided by the United States Department of Energy (Grant No. DE-FE0008868, program manager: Richard Dunst), and Indiana University – Purdue University Indianapolis Research Support Funds Grant (RSFG) and International Research Development Fund (IRDF).

REFERENCES

1. D.R. Clarke, M. Oechsner, and N.P. Padture: *MRS Bull.*, 2012, vol. 37, pp. 891–98.
2. A.G. Evans, D.R. Mumm, J.W. Hutchinson, G.H. Meier, and F.S. Pettit: *Prog. Mater. Sci.*, 2001, vol. 46, pp. 505–53.
3. D. Clarke and C. Levi: *Annu. Rev. Mater. Res.*, 2003, vol. 33, pp. 383–417.
4. R.A. Miller: *Surf. Coat. Technol.*, 1987, vol. 30, pp. 1–11.
5. R. Vaßen, M.O. Jarligo, T. Steinke, D.E. Mack, and D. Stöver: *Surf. Coat. Technol.*, 2010, vol. 205, pp. 938–42.
6. R. Vassen, X. Cao, F. Tietz, D. Basu, and D. Stöver: *J. Am. Ceram. Soc.*, 2000, vol. 83, pp. 2023–28.
7. X.Q. Cao, R. Vassen, and D. Stöver: *J. Eur. Ceram. Soc.*, 2004, vol. 24, pp. 1–10.
8. J. Zhang: *2015 NETL Crossingcutting Research Review Meeting*, Pittsburgh, PA, April 27–30, 2015.
9. J. Zhang, X. Guo, Y.G. Jung, L. Li, and J. Knapp: *Materials Today: Proceedings*, 2014, vol. 1, pp. 11–16.
10. J. Zhang, X. Guo, Y.G. Jung, L. Li, and J. Knapp: *Materials Science & Technology 2014 (MS&T)*, 2014, pp. 2061–68.
11. R. Vaßen, F. Traeger, and D. Stöver: *Int. J. Appl. Ceram. Technol.*, 2004, vol. 1, pp. 351–61.
12. P.H. Lee, S.Y. Lee, J.Y. Kwon, S.W. Myoung, J.H. Lee, Y.G. Jung, H. Cho, and U. Paik: *Surf. Coat. Technol.*, 2010, vol. 205, pp. 1250–55.
13. T.A. Taylor: US Patents No. 7910225 B2, 2011.
14. A. Bolcavage, A. Feuerstein, J. Foster, and P. Moore: *J. Mater. Eng. Perform.*, 2004, vol. 13, pp. 389–97.
15. H. Lehmann, D. Pitzer, G. Pracht, R. Vassen, and D. Stöver: *J. Am. Ceram. Soc.*, 2003, vol. 86, pp. 1338–44.
16. C. Xu, C. Wang, C. Chan, and K. Ho: *Phys. Rev. B*, 1991, vol. 43, pp. 5024–27.
17. J. Zhang, J. Yu, X. Cheng, and S. Hou: *J. Alloy. Compd.*, 2012, vol. 525, pp. 78–81.
18. H. Hayashi, T. Saitou, N. Maruyama, H. Inaba, K. Kawamura, and M. Mori: *Solid State Ionics*, 2005, vol. 176, pp. 613–19.
19. P.H. Townsend, D.M. Barnett, and T.A. Brunner: *J. Appl. Phys.*, 1987, vol. 62, pp. 4438–44.
20. X.C. Zhang, B.S. Xu, H.D. Wang, and Y.X. Wu: *Thin Solid Films*, 2005, vol. 488, pp. 274–82.
21. Y.C. Tsui and T.W. Clyne: *Thin Solid Films*, 1997, vol. 306, pp. 23–33.
22. G.K. Beshish, C.W. Florey, F.J. Worzala, and W.J. Lenling: *JTST*, 1993, vol. 2, pp. 35–38.
23. V. Viswanathan, G. Dwivedi, and S. Sampath: *J. Am. Ceram. Soc.* (2015) [10.1111/jace.13563](https://doi.org/10.1111/jace.13563).
24. C.G. Levi, J.W. Hutchinson, M.H. Vidal-Sétif, and C.A. Johnson: *MRS Bull.*, 2012, vol. 37, pp. 932–41.